NUMERICAL TOOLS DEVELOPED AT ONERA FOR THE AERODYNAMIC ASSESSMENT OF PROPELLERS AND COUNTER-ROTATING OPEN ROTORS

P. Beaumier
ONERA – The French Aerospace Lab, Meudon, France
philippe.beaumier@onera.fr

Keywords: *Propeller, Open Rotor, Aerodynamics, Performance, Installation effects*

Abstract

ONERA has developed and validated computational tools which aim at predicting the aerodynamic performance of propellers and open rotors together with the aerodynamic sources responsible for radiated noise. The objective of this paper is to discuss the strengths and weaknesses of these approaches (ranging from simple blade-element theory to 3D CFD methods), through validation against experimental data when available. It is concluded that simple methods can predict correctly the propeller performance at nominal conditions but CFD methods are required to address off-design configurations where strong unsteady effects or separated flows can appear. In particular, CFD methods are well suited to predict the unsteady aerodynamic sources of noise for an installed configuration.

1 Introduction

Open rotors have long proven their ability to reduce fuel consumption compared to turbofan engines. Motivated by the acceleration of oil prices increase and increasing environmental awareness, a renewed interest in propeller technology for future transport aircraft propulsion has grown for the last five years, leading to the consensus that Counter-Rotating Open Rotors (CROR) might be the only breakthrough technology for civil aircrafts in the 2020-2025 timeframe.

Following and sometimes anticipating the demands by aircraft and engine manufacturers, ONERA has developed and validated several computational tools which aim at predicting the aerodynamic performance of propeller driven aircrafts together with the aerodynamic sources responsible for radiated noise. These methods range from simple blade-element theory to 3D Computational Fluid Dynamics (CFD), covering a wide range of physical phenomena appearing on isolated and installed propellers and CROR. The objective of this paper is to present and discuss the strengths and weaknesses of these approaches, through specific examples of code-to-code comparisons together with validation against experimental data when available.

After a short description of the numerical methods, the first part of the paper is devoted to the prediction of aerodynamic performance for an isolated propulsive system, at nominal and off-design conditions. Then, the influence of incidence of the propeller axis is studied before discussing the methods well suited to address the complex topic of installation effects. The main findings to the analysis carried out in this paper are summarized as conclusion.

2 Numerical Methods

2.1 Blade-Element Methods (BEM)

Methods based on the Blade-Element theory are very popular because of their very low computational cost. The principle of such methods is to compute the aerodynamic sectional loads based on the sectional Mach number M and incidence α; to achieve this, 2D look-up tables are required that provide the sectional lift Cl and drag Cd coefficients of any blade section, given M and α.

Blade-Element methods differ by the way the wake system generated by the lifting surfaces (blades) is modeled. Based on incompressible assumption, the wakes are generally modeled by singularities (filaments or panels), the Biot&Savart law being then used to compute the velocities induced by the wake system at each blade section. Two codes using such a Blade-Element approach are briefly described below.

2.1.1 Quasi-Steady Wake Model: LPC2

In the LPC2 code developed in the 80's by ONERA [1], the wake of each blade is modeled by a set of vortex lattices (Fig. 1, left), the circulation of which is deducted from the sectional loads on the emitting blade. The geometry of each lattice is helical, with a pitch which is iteratively computed for consistency with the sectional loads, in a quasi-steady approach.

Note that the wake model and hence the induced velocities computed by LPC2 are only valid in axial flight conditions, when the propellers have zero incidence, for an isolated single propeller or CROR. In the case of CROR, the mutual induced velocities (defined as the velocities induced by the wake of one propeller on the blade sections of the opposite propeller) are systematically computed (both axial and swirl velocities).

Moreover, an option can be used in the LPC2 code in order to account for non uniform free stream perturbations, through a correction of the sectional velocities as a post-treatment: in such a case, the wake is not re-computed and the induced velocities of the undisturbed configuration are used instead, which can be a crude assumption. Calculation results using this option will be labeled as "LPC2 with installation effect" in the next sections.

2.1.2 Unsteady Free-Wake Model: MINT

The free-wake model MINT was initially developed by ONERA for helicopter applications [2][3]. It mainly differs from the wake model used in LPC2 by the following features:

- The type of singularities used: panels with low order singularity (instead of lattices),
- Time-marching approach, which means that any kind of unsteady conditions can be computed with the MINT code.

MINT belongs to the so-called "free-wake" models meaning that at each time step the velocities induced by the whole vortex system are computed at each collocation point in order to distort the edges of each panel (Fig. 1, right).

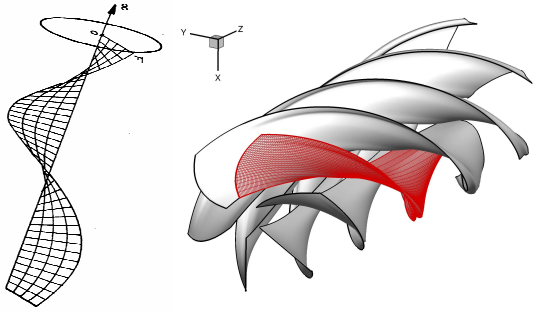

Fig. 1. Wake Model used in LPC2 (left) and MINT (right)

2.2 RANS Methods

Reynolds-Averaged Navier-Stokes (RANS) methods solving the general fluid mechanics conservation equations are now very popular and mature for any kind of aeronautical applications. All the simulations presented below were obtained using the ONERA in-house *elsA* CFD solver [4][5], generally used with the adjunction of a 2 equation turbulence model such as k-ω Kok (low Reynolds modelization). The e*lsA* code makes use of multiblock structured meshes with a wide range of possibilities for the connectivity between blocks (coincident, partially non coincident, totally non coincident, overlapping).

2.2.1 Actuator Disk Approach

The easiest way to account for the influence of a propeller in a flow is to simply model the propeller by an internal boundary condition, often called "actuator disk", through for example the adjunction of source terms which model the force jumps (pressure and tangential components) brought by the rotating blades in the momentum and energy equations (the turbulent equations being unchanged as a first

approximation). This quasi-steady method requires the 3-component forces distribution on the propeller disk as an input, which can be provided by the LPC2 method described above. It allows having a first idea on how the propeller modifies the flow, but is not well suited to assess the propeller performance, since the rotating blades are not included in the CFD mesh.

2.2.2 Azimuthal Reduction

For some specific flow conditions, computing a propeller or a CROR does not require the meshing of the whole configuration including each rotating blade. The symmetry of the flow or the application of specific boundary conditions can be used to make an azimuthal reduction, which means, for each propeller with N-blades, that a simulation on only an azimuthal sector of $2.\pi/N$ can be done.

The first trivial application of this kind of reduction is the simulation of a single isolated propeller in axial flight, for which periodicity conditions on the pitchwise boundaries can be used. Slightly more complex, a so-called "mixing-plane" (MxPL) boundary condition can be applied on the boundaries between the blocks of the front and aft propeller blades, in addition of periodicity conditions on the pitchwise boundaries, in order to simulate an isolated CROR in a quasi-steady approach (Fig. 2): unsteady effects are omitted through the average of flow quantities exchanged at the interface between the propellers, but averaged interaction effects are expected to be captured.

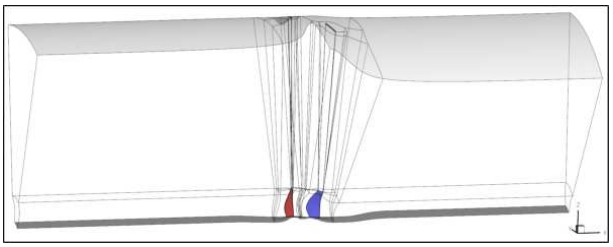

Fig. 2. CFD mesh topology for a reduced approach on a CROR (mixing plane or chorochronic)

A second application consists in the unsteady simulation of an isolated CROR in axial flight. In this case, only 1 channel around one blade of the front and one on the aft propeller is modeled, and a phase-lag method with chorochronic boundary conditions can be used [6]. Such boundary conditions take advantage of the fact that the solution at one point of the boundary between the two propellers (or between two blades) at a given time t is the same as the solution that was obtained at the same relative location but at a retarded time t', the time shift being directly related to the passage frequency of the blades belonging to the two propellers (single frequency approach). An extension of this technique to multi-frequency problems to tackle for example the interaction between a pylon and a CROR has been recently developed in *elsA*, named as multi-chorochronic method [7].

2.2.3 Full Annulus 360° Approach

When no approximation on the flow physics can be done, a complete approach called "full annulus or 360" has to be used. It requires the meshing of all solid surfaces in a complex grid system comprising both rotating and non-rotating parts. An example of the meshing strategy used at ONERA is given in Fig. 3: the blocks rotating with the front propeller are drawn in red while the blocks rotating with the aft propeller are in blue. Both classes of blocks are embedded in a background grid system, which is fixed in time (black grid), and the Chimera technique is used at each time step to ensure information transfer between the different blocks. Any other component of the configuration can then be easily added, such as an upstream pylon or even a fuselage.

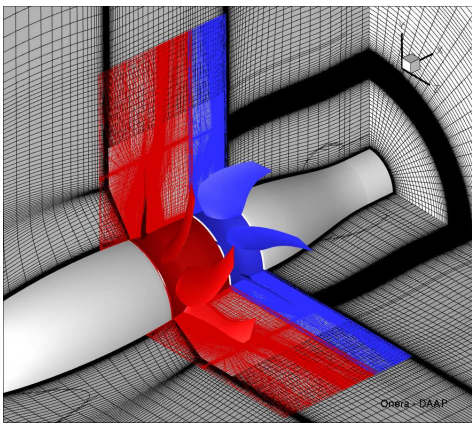

Fig. 3. Example of meshing strategy for full annulus 360 calculations

3 Performance Prediction of Isolated Propulsive System

In this part, it is assumed that the propulsive system, propeller or CROR, is isolated (the presence of an axisymmetric spinner can be added to the propeller blades), operates in axial flight (no incidence, axisymmetric free-stream conditions) and that the blades of a given propeller all have the same geometric characteristics (isotropy). The objective is to evaluate the ability of the different numerical methods described above to predict the propeller performance, which can be assessed on the following quantities:

- Propeller thrust coefficient, $C_t = \frac{T}{\rho_0 N^2 D^4}$

- Propeller power coefficient, $C_p = \frac{P}{\rho_0 N^3 D^5}$

- Propulsive efficiency (Eta), $\eta = \frac{T.V_0}{P}$

T is the propeller thrust, P the power, V_0 the advancing velocity, D the propeller diameter and N the propeller rotating frequency.

Most of the cases investigated below are extracted from the DREAM European project, during which several CROR designs were experimentally tested in the TsAGI wind-tunnels both in low speed (advancing Mach number M~0.25, Fig. 4) and high speed conditions (M~0.78). More information about this database can be found in [8].

Fig. 4. VP-107 Test Vehicle in TsAGI Low Speed T-104 Wind Tunnel (DREAM project)

3.1 Nominal Conditions

At M=0.25, for nominal flight conditions reproducing how a CROR would operate at Take-Off, both BEM and CFD methods are able to predict the propeller performance with a reasonable accuracy close to 10% for CFD and close to 15% for the BEM method, as illustrated in Fig. 5, where the coefficients are normalized by their experimental value (experiment=100%). For this configuration of a 12-10 bladed design called V0, the LPC2-BEM code does a very good job in the prediction of the front propeller performance (red bars), but largely underestimates the aft propeller thrust and power coefficients. *elsA*-CFD overestimates thrust and power for the two propellers (blue bars). In the end, the efficiency is computed within 5% accuracy, which is acceptable. The comparison between the two CFD results in Fig. 5 is interesting (blue and purple bars) since it allows quantifying unsteady effects: the results in purple correspond to the average value of the performance extracted from an unsteady calculation using the chorochronic approach. Since the two CFD results are very close, it can be concluded that a simple quasi-steady approach using the mixing-plane technique is sufficient for the prediction of performance.

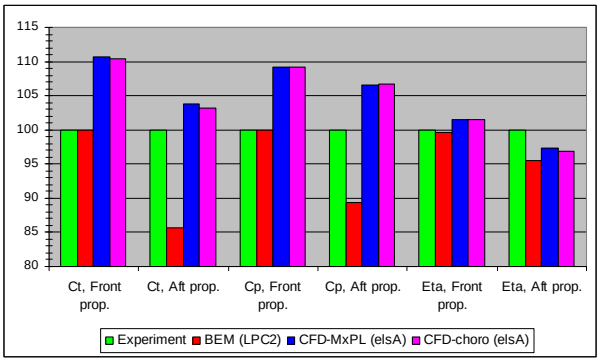

Fig. 5. Performance Prediction at Low Speed for Nominal Conditions

It can be shown that the BEM results can be slightly improved if the influence of the test rig (modeled through non uniform free stream velocities in the radial direction: “installation effects”) is accounted for, reducing the deviation from experimental values from 15% to 10%. Of course, the use of CFD instead of BEM is computationally more expensive but gives access to much more information on the

physics in the flow field, and very nice comparisons on the Mach number or total pressure radial distributions behind the aft propeller have been obtained (more details can be found in [9]).

During the same DREAM project, several CROR designs were tested in the same TsAGI facility for similar flight conditions. A key question is to know whether the numerical methods are able or not to predict the gain (or loss) of performance of a design compared to a reference design. This exercise is done in the same low speed condition as above, comparing a so-called V1.1 CROR design to the V0 design used as a reference. In the experiment, an efficiency improvement was measured on both front and aft propellers, by respectively 16% and 7% (green bars in Fig. 6). The LPC2-BEM method predicts only a very small improvement of the front propeller efficiency (red bars), while the *elsA*-CFD mixing plane method predicts the performance improvement quite accurately. The origin of the poor accuracy of the BEM method in this case lies probably in the accuracy of the 2D look-up tables used to generate these results, while the use of CFD is straightforward to compute such trends dominated by 3D effects.

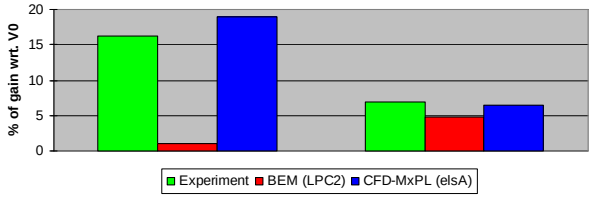

Fig. 6. Efficiency Modification of the DREAM V1.1 Design Compared to the Reference Design V0. Left: Front Propeller. Right: Aft Propeller

In cruise flight (M=0.73) the aerodynamic conditions are characterized by strong transonic effects. Indeed, the helical Mach number in these conditions, which combines the effect of blade rotation and advancing velocity, is close to 1 at the blade tip. Globally speaking, Fig. 7 shows that CFD provides more consistent results compared to experiment than BEM. However, the deviation from experiment are larger than in the low speed case, with an accuracy on thrust and power coefficients which can be more than 20% for BEM and around 10 to 15% for CFD. The propeller efficiency is predicted within a range of 10 to 15%. Taking into account the test rig installation effects has a beneficial effect in the accuracy of the BEM method which then becomes close to the one of the CFD method (not shown here, see [9]).

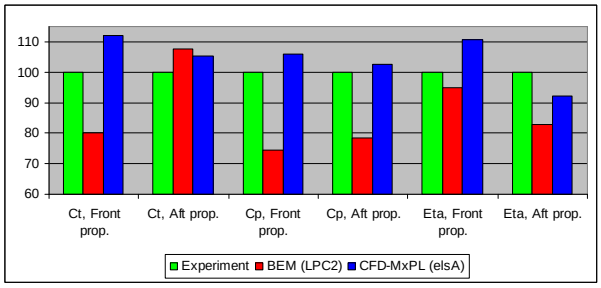

Fig. 7. Performance Prediction at High Speed for Nominal Conditions

3.2 Off-Design Conditions

The conditions investigated in this part do not pretend to be exhaustive, and only a selection of off-design conditions is presented in the two following paragraphs, focusing on the influence of RPM reduction at low speed and on the challenging configuration of reverse conditions.

3.2.1 RPM sweep

A set of four data points was acquired during the DREAM low speed tests, starting from the nominal point (§3.1) and decreasing simultaneously both propeller RPMs. Measurements were performed for RPM ranging from 60% to 100% of nominal RPM.

Fig. 8 shows the RPM effect on global coefficients for front and aft propellers using LPC2-BEM without and with installation effects (averaged perturbations from the test rig). The overall trends seem to be well captured on both propellers. Absolute values on the front propeller are also well estimated since the error between experiment and computation is less than 10%, reducing around 5% when accounting for installation effects. Discrepancies seen on the absolute values are much higher on the aft propeller. Only the low RPM computation (60% nominal RPM) shows important discrepancies on the aft propeller. When looking more into details (not shown here), it can be seen that in such a configuration, the aft blade root is in a deeply stalled condition according to 2D airfoil look-up tables. Blade stall could also be forecast

when looking at experiment (loss in both thrust and efficiency) but to a much lower extent. Accounting for installation effects greatly improves this point. Since LPC2 does not account for any hub line geometry, an important part of the blade does not see the true local Mach number due to the bulb and the hub geometry change. At high RPM, the local flow field at a blade section is dominated by the RPM and moreover, the blade works far away from the stall region. Therefore a slight change in local Mach number does not affect that much the airfoil characteristics. But at low RPM accounting for the true local Mach number seems mandatory.

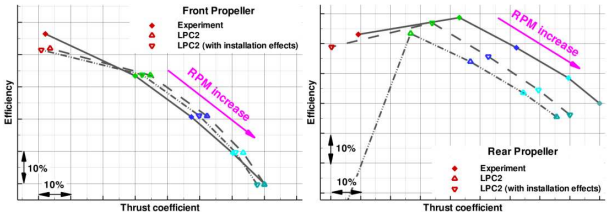

Fig. 8. RPM Effect on Efficiency. BEM Method (LPC2)

Fig. 9 shows the RPM effect on global coefficients for front and aft propellers using *elsA*-CFD without and with installation effects. Surprisingly, CFD computation does not seem to be as accurate as the lifting-line method on the front propeller. The increase in efficiency as RPM is decreased is correctly captured, but the absolute values are higher in the CFD computation than in experiment. Accounting for installation effects slightly improves the absolute values but does not recover all the discrepancy. However, the aft propeller computation seems to be more accurate, with very close values between experiment and CFD. The low RPM point (60% nominal value) features some stall behavior in both CFD and experiment. Comparison is even improved when accounting for installation effects.

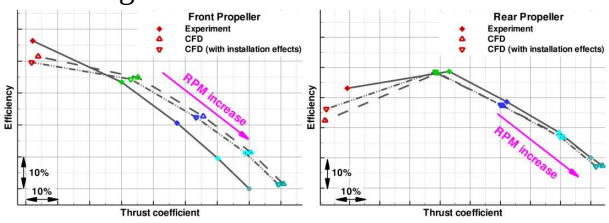

Fig. 9. RPM Effect on Efficiency. CFD-MxPL Approach (*elsA*)

A more detailed assessment of the ability of CFD to capture RPM effects is provided in Fig. 10, which shows an accurate comparison with experimental results, as far as the Mach number and total pressure radial distributions after the aft propeller are concerned.

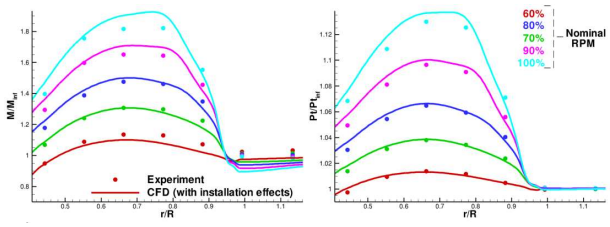

Fig. 10. RPM Effect on Mach Number and Total Pressure Distributions Behind the Aft Propeller with a CFD-MxPL Approach (*elsA*)

3.2.2 Reverse conditions

Reverse conditions stand for conditions in which the propeller thrust is directed in the same direction as the free stream, which means that the induced flow field across the propeller is directed opposite to the free stream. This means that the average axial velocity is reduced through the propeller, instead of being increased in nominal conditions. This configuration can be used at landing to ease the airplane deceleration. Depending on the relative values of the free stream and the propeller axial induced velocities, the resulting flow field can be quite different. Since the axial induced velocity is directly related to the propeller thrust and is also a function of the free stream velocity, there are a priori several parameters to be investigated to better understand the physics of reverse conditions.

Using 1D momentum theory allows defining a reduced thrust coefficient τ^* as: $\tau^* = \frac{T}{1/2\rho_0 S V_0^2}$, where S is the propeller disk area. According to this theory:

- If $\tau^* < 1$: the flow field remains stable
- If $\tau^* > 1$: the flow field can be unstable, unless τ^* becomes very large compared to 1

In order to better understand what happens, CFD simulations using an actuator disk approach have been carried out on a single

propeller in low speed conditions (M=0.2) and varying the pressure jump across the rotor disk in order to study different values of the τ^* coefficient, ranging from 0.8 to 4. The resulting flow field is illustrated in Fig. 13 where the streamlines in black are superimposed to the Mach number contours (main flow field is directed from left to right). For low τ^* values, the propeller induced velocity is not strong enough to significantly modify the flow field: in other terms, the free stream is strong enough to have streamlines always directed from left to right. Note however that this is indeed a reverse condition by looking at the blue colors indicating flow deceleration behind the propeller. For $\tau^* > 1$, recirculating flow starts to appear, first in the propeller wake downstream the propeller disk, and progressively moving upstream as the propeller induced velocity is becoming stronger and generates more opposition to the free stream. For $\tau^* \sim 2$, this recirculation area is right in the plane of the propeller disk and the flow is deviated beyond the propeller blade tips in the radial direction before coming back more inboard and crossing the propeller from right to left, which means opposite to the main free stream. One can guess that this condition, close in nature to the well-know Vortex Ring State (VRS) for helicopters, is quite unsteady in nature. For very large values of τ^*, the recirculation area is moved upstream the propeller disk.

In order to progress in the analysis, CFD simulations modeling the rotating blades have been done, first using a steady approach and then a time consistent approach, for a typical reverse condition at M_0=0.2. In this case, the propeller blade pitch angle was set to a negative value provided by industry, and the results of these simulations provided an average propeller thrust leading to a reduced coefficient $\tau^* \sim 1.2$. The comparison of the flow field for these two simulations with the one done using the actuator disk approach shows some nice qualitative similarities (Fig. 11), especially concerning the shape and the position of the area of recirculating flow.

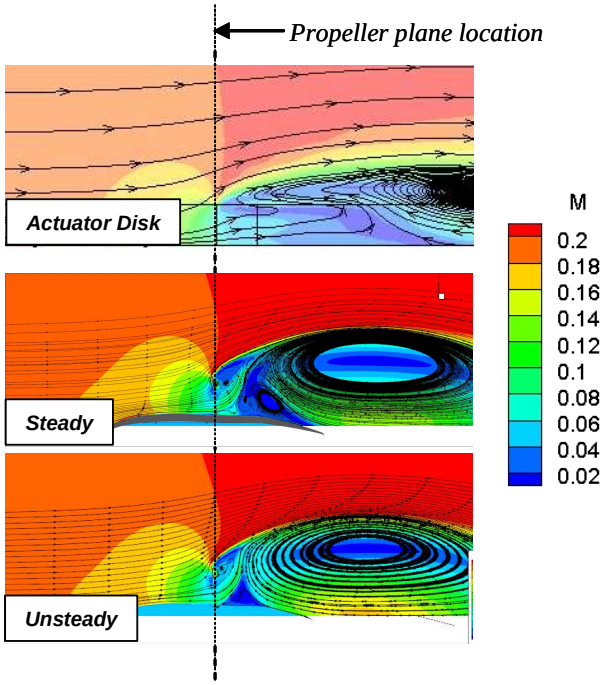

Fig. 11. Influence of Numerical Modeling on the Flow Field in Reverse Condition

The detailed analysis of the numerical solutions reveals that it is difficult to reach a good convergence, each calculation (steady or unsteady) providing oscillating results both in terms of residuals and of integrated quantities such as propeller thrust. This confirms the probable unsteady if not unstable character of this flight condition, probably emphasized by large area of flow separation on the blade as shown is Fig. 12.

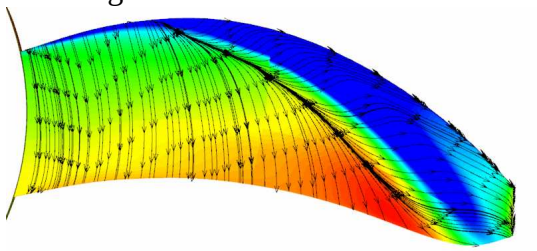

Fig. 12. Skin Friction Lines on a Blade for a Propeller in Reverse Condition: Visualization of Flow Separation

Further work is still required to address this challenging reverse configuration as was already initiated by Snecma using the *elsA* code [10]. Detailed experimental results will be needed to assess the accuracy with which numerical methods can predict the propeller blade loads in such flight conditions.

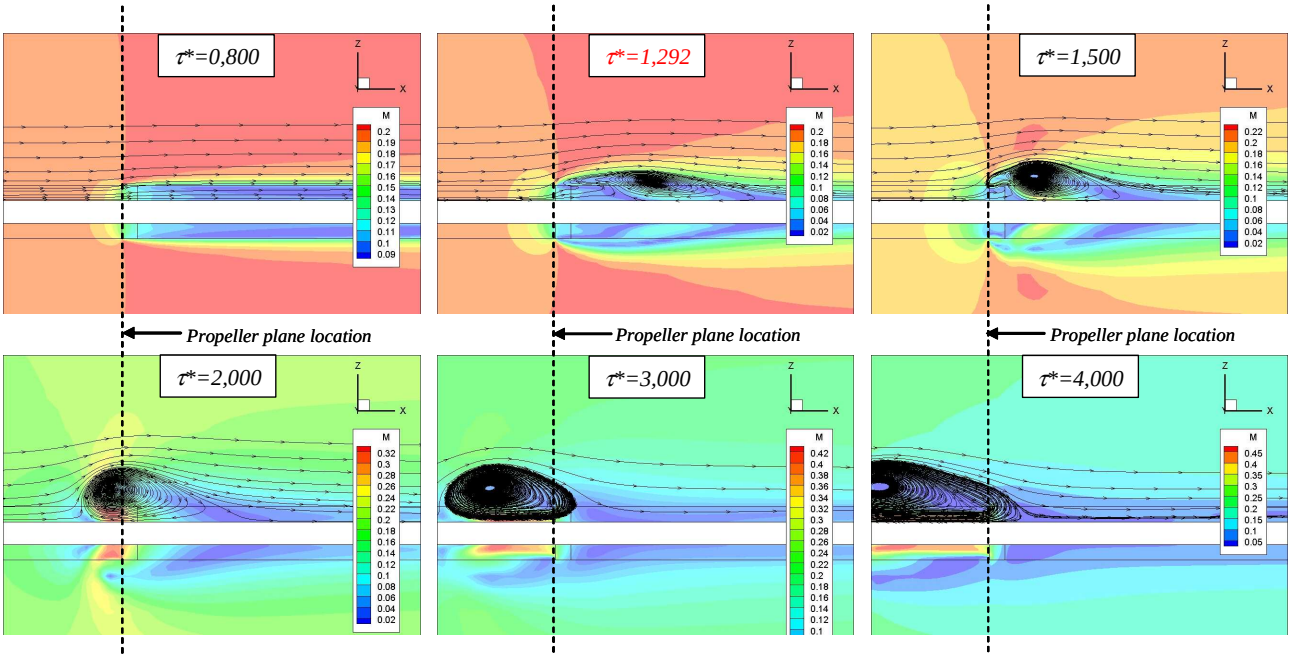

Fig. 13. Flow Field in Reverse Conditions Simulated by an Actuator Disk Approach (Single Propeller).

4 Effect of Incidence: 1P loads

When the air stream entering the propeller disk has some angle (incidence) with respect to the thrust direction (propeller angle of attack), the blades generate aerodynamic forces that vary cyclically over one revolution. As a result, the net force over the propeller is no longer purely axial (thrust), but is also composed of in-plane loads (1P). Predicting accurately the 1P loads is necessary for structural design: 1P loads may present a mean value constraining the static sizing. Likewise, their frequency and amplitude have a great influence on structural fatigue and cabin comfort (vibration).

The European project APIAN provides an extensive experimental database for an isolated, 6-bladed transonic propeller tested at various angles of attack, Mach numbers and RPM conditions (Fig. 14), covering a large part of the flight domain (from take-off at M=0.2 to cruise conditions at M=0.7). A brief summary of the detailed analysis of 1P loads on this configuration done in [11] is proposed hereafter.

Fig. 14. APIAN Propeller in S1MA Wind-Tunnel

The physics behind the vertical component of the 1P loads is quite straightforward: the downward moving blade experiences greater angles of attack and velocities than the upward moving blade. Thus, it generates more lift and drag. The vertical projection of these two forces on the rotation plane is superior to that of the upward moving blade. The resulting net force over the entire propeller is directed upwards (positive Fz). The origin of the lateral 1P loads is more complex and lies in the dissymmetry of the velocities induced by the wake system: contrary to the vertical 1P loads, where the dissymmetry concerns the right-left parts of the propeller disk, here the dissymmetry concerns the upper/lower parts of the propeller disk. It is

believed that this dissymmetry is largely due to unsteady aerodynamics. This assumption is confirmed by the fact that a quasi-steady BEM method like LPC2 is unable to predict this lateral component of 1P loads. On the contrary, recent studies which are still on-going indicate that the unsteady model present in the MINT wake model allows a reasonable prediction of 1P loads [12]. However, today, the most accurate way to predict 1P loads is to perform CFD unsteady RANS (URANS) simulations.

It has first been shown that grid refinement has a significant effect on the prediction of the blade loads. To give orders of magnitude, the so-called baseline grid comprises a total of 18M points, this number being increased to 40M points in the fine grid. Globally, a good agreement is found between the predictions and the APIAN measurements: the pressure peak near the leading-edge is better captured with the fine grid compared to experiment, especially in the low speed M=0.2 case, as illustrated in Fig. 15 and Fig. 16, for a blade section located at 65% in the spanwise direction.

It is then interesting to assess the accuracy of CFD methods in predicting the 1P loads. This is done below in the low speed case, all results including the high speed case being detailed in [11]. The vertical component of the 1P loads is plotted in Fig. 17 as a function of the propeller incidence. Note that this vertical component is expressed as a percentage of the propeller axial thrust. The linear behaviour of the curve is well reproduced by the CFD calculation, with a slope which is slightly underestimated. Using the fine grid has no influence in the value of the vertical 1P load (1 calculation done for the 15° incidence).

Although of lesser amplitude than the vertical component, the lateral component of the 1P load is correctly estimated too (Fig. 18). Here, grid refinement tends to reduce the discrepancy between predictions and measurements for the highest incidence angle 15°.

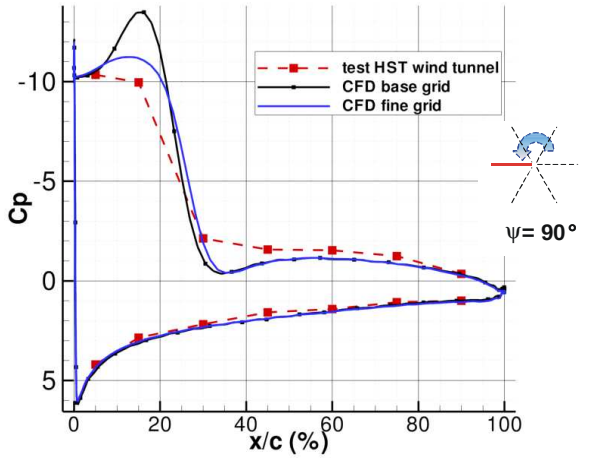

Fig. 15. Pressure Distribution on the APIAN Propeller. Low speed (M=0.2), Incidence=15°. ψ=90° (Advancing Side)

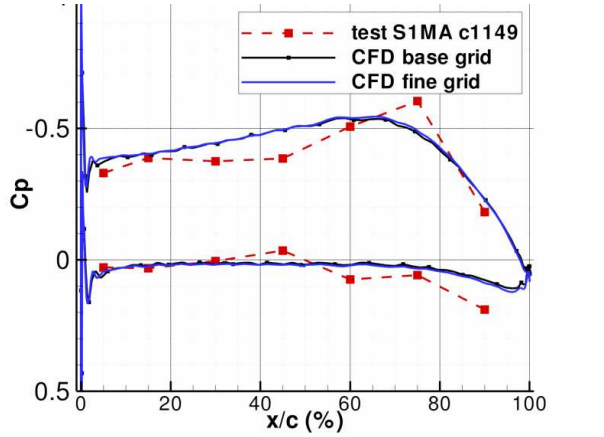

Fig. 16. Pressure distribution on the APIAN propeller. High speed (M=0.7), Incidence=3°. ψ=90° (advancing side)

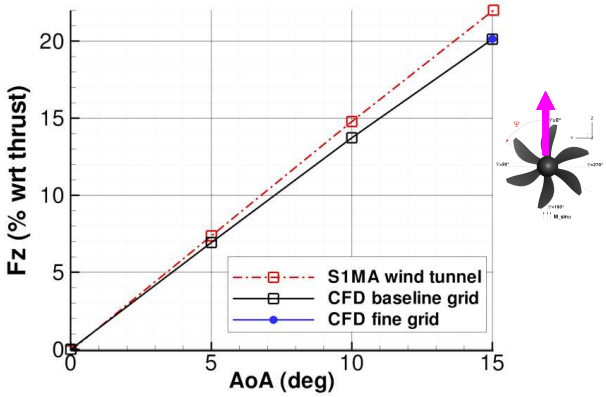

Fig. 17. 1P Vertical Load on the APIAN Propeller at Low Speed (M=0.2)

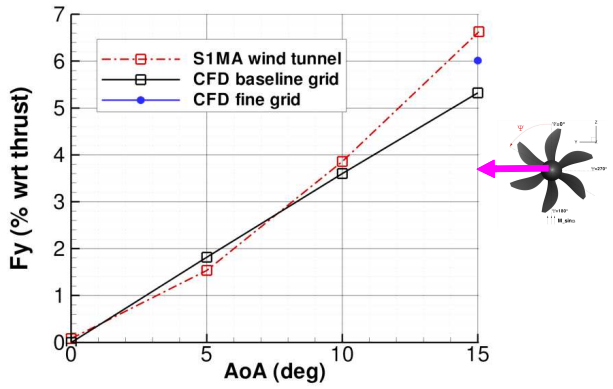

Fig. 18. 1P Lateral Load on the APIAN Propeller at Low Speed (M=0.2)

Still, some discrepancies remain between predictions and measurements of the 1P loads. As shown in [11], one part of these discrepancies come from the fact that the measured loads included the loads acting on the rotating part of the spinner, whose in-plane components are not equal to zero because of the non symmetric influence of the propeller loads. Indeed, adding to the computed values the loads generated by the spinner provides a better estimation of the measured 1P loads (red diamond in Fig. 19).

Globally speaking, for the APIAN single propeller, it has been found that vertical 1P loads could be predicted by CFD with accuracy better than 10% and lateral loads with accuracy better than 5%, which is quite satisfying.

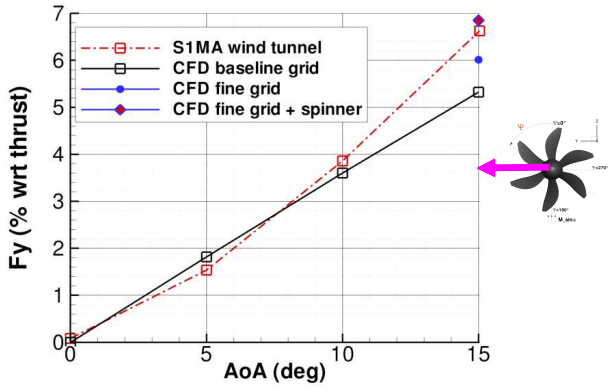

Fig. 19. Influence of Spinner on the 1P Lateral Load at Low Speed (M=0.2)

5 Installation Effects

Being able to predict accurately installation effects for a single propeller or a CROR remains a challenge that requires the use of advanced and heavy numerical simulations. Two problems have to be addressed:

- What is the impact of the installation (pylon, fuselage …) on the propellers? This influence has to be quantified in terms of steady loads (performance: thrust and power) as well as unsteady loads which are responsible for noise emission;
- What is the impact of the propellers on the airframe? This comprises the vibrations transmitted by the propulsive system to the fuselage as well as the noise generated by the rotating blades, both in the near field and in the far-field.

Taking advantage of the quite complex installation studied in the DREAM project (Fig. 4), ONERA has been computing the full configuration illustrated in Fig. 20 by performing a full unsteady time-accurate simulation of one of the CROR geometries tested in TsAGI, taking into account most of the solid elements surrounding the propellers. The complex grid system comprised a total of more than 200M points. Restitution time for one propeller revolution was approximately 235 hours (computation distributed over 256 Nehalem-EP - 2.8Ghz - processors). More details about this unique simulation can be found in [13][14].

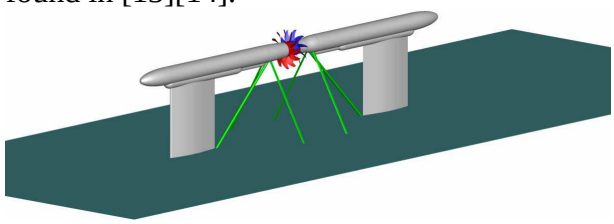

Fig. 20. DREAM Geometry Used in the *elsA* URANS Simulation

5.1 Influence on performance

The numerical solution exhibited quite significant unsteady effects, in terms of unsteady blade loads or unsteady variations of total pressure or swirl angle measured by rakes

located behind the aft propeller, as illustrated in Fig. 21. Although the frequency of the unsteadiness is not always linked to the blade passing frequencies, it is quite interesting to notice that the time average of these unsteady fluctuations:

- Agree quite well with steady measurements,
- Are very close to the computational results obtained by a steady calculation (MxPL) on the isolated CROR (w/o installation effects).

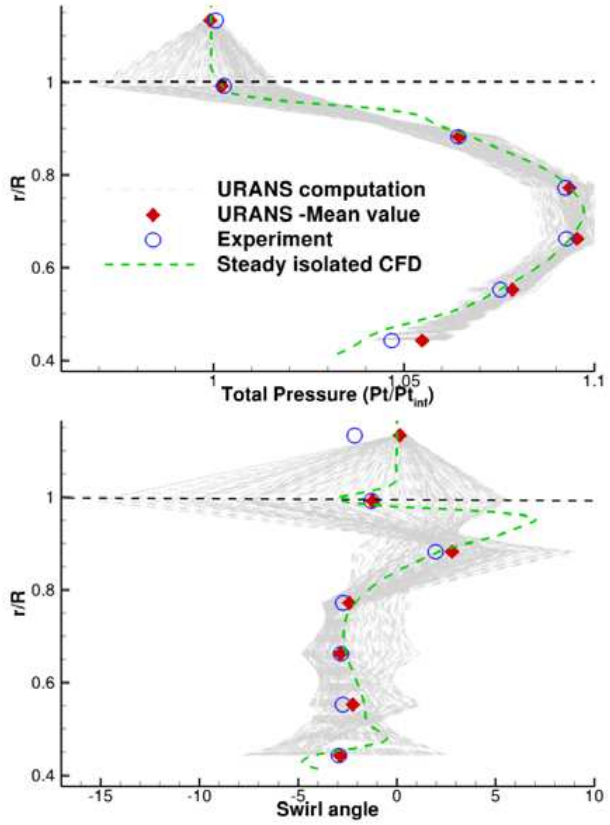

Fig. 21. Downstream Rakes Deviation (CFD vs. DREAM Experiment)

Finally, the time-averaged performance of the propellers are extracted from the installed unsteady calculation and compared to the performance of the isolated CROR. The front propeller thrust and power coefficients were found to be from 5 to 6% higher with installation effects (*elsA*-360 calculation) than without (*elsA*-MxPL calculation); similarly, the aft propeller thrust and power coefficients were found to be 3% higher with installation effects. This leads to a small, although not negligible, impact on the propeller efficiency which is reduced by 0.5 to maximum 1 count when installation effects are accounted for.

5.2 Influence on acoustics

Before running an acoustic computation it is always interesting to have a look at the density gradients in the flow field since it is representative of the "acoustic waves". An instantaneous snapshot of the density gradient distribution is shown in Fig. 22.

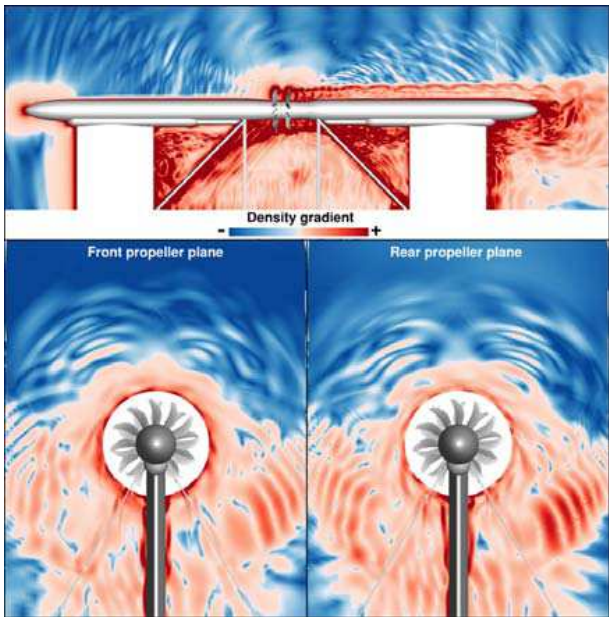

Fig. 22. Density Gradient Distribution from the Installed URANS Simulation

In addition to the large gradient values in all the regions dominated by vortical flow (downstream the pylon, downstream the propeller…), what is interesting, acoustically speaking, is the regions of small gradients values, which evolve in coherent fronts. Those are time dependent and usually coherent with the blade passing frequencies and their harmonics. Such waves are clearly visible on the upper part of the test rig (upper figure), moving both upstream and downstream the propellers planes. The same waves are also visible in the plane of the propellers (lower figures). While these waves are typical of a propeller, some others like the two lateral waves in the propeller plane seem to come from below the rig due to installation effects.

The unsteady wall pressure distribution from the CFD computation is used to compute

the tone noise radiated in the far field by the open rotors but also the noise radiated by the test rig itself. To do this, the KIM code is used [15], based on acoustic integral methods and solving the Ffowcs Williams Hawkings (FW-H) solid surfaces equation in the time domain. In order to better understand the physics, the acoustic radiation was done:

- First by radiating the fluctuations generated by the propellers alone
- Then by radiating the fluctuations generated by the test rig alone
- Finally using all solid surfaces

It can be seen in Fig. 23 that the calculation successfully predicts the level and directivity of the propeller fundamental tones (BPF1 and BPF2). Note the significant contribution of the radiation of the rig on the global level of the aft propeller fundamental BPF2. The interaction tone BPF1+BPF2 is quite well predicted too.

This nice comparison between the unsteady installed calculation and experiment shows that the global effect of the test rig on acoustics is captured in the computation. Such a good agreement is impossible to reach if only an unsteady calculation of the isolated CROR is done (w/o installation effects), especially as far as the fundamental harmonics BPF1 and BPF2 are concerned.

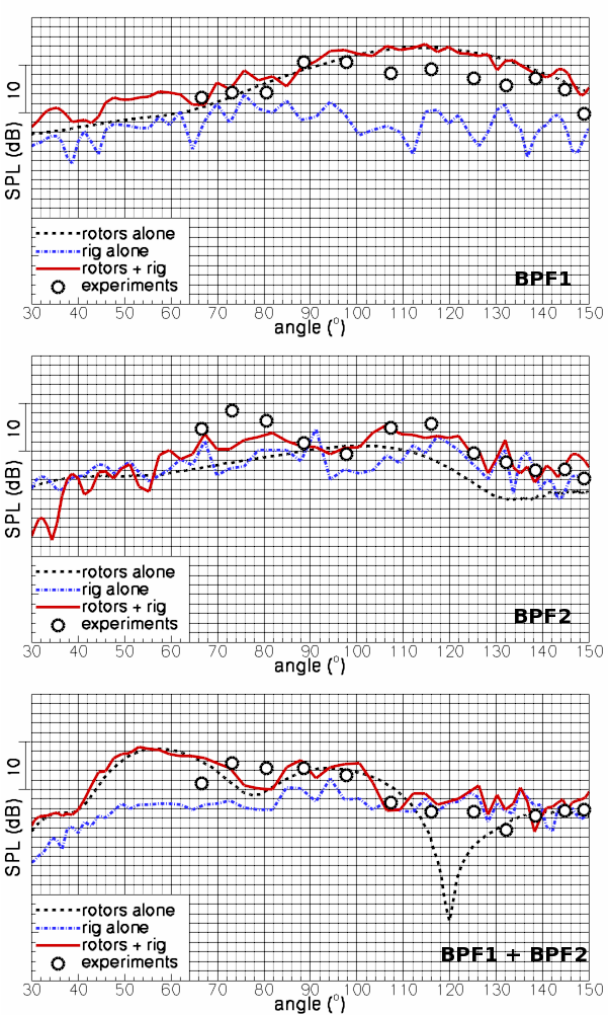

Fig. 23. Tones Directivities (CFD Installed Calculation vs. Experiment)

6 Conclusion. Future Work

A variety of numerical methods have been applied by ONERA on open rotor configurations, ranging from simple BEM codes (which can be run in a few seconds on a PC) to unsteady RANS codes which can require several thousand hours of CPU time on a super computed for installed configurations. Each of these methods has its own advantages and drawbacks and has to be used in a smart way depending on the physics to be investigated.

From the validations carried out currently, the main following conclusions can be drawn:

- For aerodynamic performance prediction in nominal conditions, both BEM and CFD methods do a pretty good job: similar accuracy in the 5 to 10% range is achieved, when mean installation effects (non homogeneous far field conditions) are applied.

- CFD does better than BEM codes to assess the performance benefits brought by a new CROR design compared to a known reference.

- Steady calculation for aerodynamic performance prediction is sufficient; installation effects have a limited although non negligible impact on performance (1 count of efficiency at nominal conditions).

- For performance in off-design conditions, often characterized by area of flow separation, it

is preferable to use CFD, which is more predictive than BEM codes.

- 1P loads appearing on a propeller in incidence can be reasonably well predicted by any method accounting for unsteady effects. Today, CFD seems to be the most accurate method, but unsteady vortex methods are very promising.

- The tone noise radiated by the isolated propellers in axial flight can be assessed using CFD with azimuthal reduction. Only huge CFD URANS calculations can predict the influence of installation effects on the propeller fundamental tones BPF1 and BPF2 with a good accuracy.

Future work is still needed in order to reach methods which can be used routinely with sufficient confidence. The main perspectives concern:

- The validation of installed and off-design configurations, which require well documented and good experimental results, both for aerodynamics and acoustics.

- The development of intermediate methods through different kind of coupling strategies between BEM and CFD codes. The main objective is to reduce the computation effort, while keeping the most important physics in the methods.

References

[1] Gardarein P. Calculs aérodynamiques des hélices rapides transsoniques. *28ème colloque d'aérodynamique appliquée*, Saint Louis, France, 21-23 octobre 1991

[2] Le Bouar G, Costes M et al. Numerical simulations of unsteady aerodynamics of helicopter rotor in manoeuvring flight conditions. *Aerospace Science and Technology Journal*, 2004

[3] Rodriguez B. Blade Vortex Interaction and Vortex Ring State captured by a fully time marching un-steady wake model coupled with a comprehensive dynamics code", *Heli Japan Conference 2010*

[4] Cambier L et al. An Overview of the Multi-Purpose *elsA* Flow Solver", *Aerospace-lab Journal*, Issue 2, Mars 2011, http://www.aerospacelab-journal.org

[5] Reneaux J, Beaumier P and Girodroux-Lavigne P. Advanced Aerodynamic Applications with the *elsA* Software, *Aerospace-lab Journal*, Issue 2, Mars 2011, http://www.aerospacelab-journal.org

[6] Erdos J.I, Alzner E and McNally W. "Numerical Solution of Periodic Transonic Flow Through a Fan Stage", *AIAA Journal*, Vol. 15, No. 11, 1977, pp. 1559–1568

[7] Castillon L. Evaluation of a multiple frequency phase lagged method for unsteady numerical simulations of multistage turbomachinery configurations, *28th ICAS conference*, Brisbane, September 2012

[8] V. Pankratov I.V. Acoustic tests of contra rotating propellers in the Dream project, *17th AIAA/CEAS Aeroacoustics Conference*, Portland, Oregon, June 2011

[9] Boisard R, Delattre G and Falissard F. Assessment of Aerodynamics and Aero-Acoustics Tools for Open Rotors. *9th ETC Conference*, Istambul, Turkey, March 21-25, 2011

[10] C. Dejeu C, Vernet M and Talbotec J. Reverse thrust tests: an experimental approach based on numerics. *3AF Symposium of Applied Aerodynamics*, Paris, March 26-27-28, 2012

[11] Ortun B, Boisard R and Roulland S. Assessment of propeller 1P Loads Predictions. *46th Symposium of Applied Aerodynamics*, Orléans, France, March 28-30 2011.

[12] Gonzalez-Martino I, Costes M, Rodriguez B and Devinant P. Application of an Unsteady Curved Lifting-Line Theory to Propeller Simulations, *30th AIAA Applied Aerodynamics Conference*, New Orleans, 25-28 June 2012.

[13] Boisard R, Delattre G and Falissard F. *ElsA* HPC capabilities applied to a counter rotating open rotor test rig. *3AF Symposium of Applied Aerodynamics*, Paris, March 26-27-28, 2012.

[14] Falissard F, Boisard R and Delattre G. Aeroacoustic Computation of a Contra Rotating Open Rotor Model with Test Rig Installation Effects, *18th AIAA/CEAS Aeroacoustics Conference (33rd AIAA Aeroacoustics Conference*), 4-6 June 2012, Colorado Springs, CO

[15] Prieur J. and Rahier G. Aeroacoustic integral methods, formulation and efficient numerical implementation. *Aerospace Science and Technology Journal*, Vol. 5, 2001, pp. 457–468

Copyright Statement